3-2013

Antioxidant Treatment Regulates the Humoral Immune Response during Acute Viral Infection

Katie E. Crump
Wake Forest University School of Medicine, kcrump@nova.edu

P. Kent Langston
Wake Forest University School of Medicine

Sujana Rajkarnikar
Wake Forest University School of Medicine

Jason M. Grayson
Wake Forest University School of Medicine

JVI Journals.ASM.org

Antioxidant Treatment Regulates the Humoral Immune Response during Acute Viral Infection

Katie E. Crump, P. Kent Langston, Sujana Rajkarnikar, Jason M. Grayson

Department of Microbiology and Immunology, Wake Forest University School of Medicine, Winston-Salem, North Carolina, USA

Generation of reactive oxygen intermediates (ROI) following antigen receptor ligation is critical to promote cellular responses. However, the effect of antioxidant treatment on humoral immunity during a viral infection was unknown. Mice were infected with lymphocytic choriomeningitis virus (LCMV) and treated with Mn(III)tetrakis(4-benzoic acid)porphyrin chloride (MnTBAP), a superoxide dismutase mimetic, from days 0 to 8 postinfection. On day 8, at the peak of the splenic response in vehicle-treated mice, virus-specific IgM and IgG antibody-secreting cells (ASC) were decreased 22- and 457-fold in MnTBAP-treated animals. By day 38, LCMV-specific IgG ASC were decreased 5-fold in the bone marrow of drug-treated mice, and virus-specific antibodies were of lower affinity. Interestingly, antioxidant treatment had no effect on the number of LCMV-specific IgG memory B cells. In addition to decreases in ASC, MnTBAP treatment decreased the number of functional virus-specific $CD4^+$ T cells. The decreased numbers of ASC observed on day 8 in drug-treated mice were due to a combination of Bim-mediated cell death and decreased proliferation. Together, these data demonstrate that ROI regulate antiviral ASC expansion and have important implications for understanding the effects of antioxidants on humoral immunity during infection and immunization.

Antibodies are a critical component of the immune system's defense to infectious microorganisms. In order to initiate an antibody response to a pathogen, naïve B cells must first be activated through recognition of antigen by the B cell receptor (BCR). Following antigen stimulation, activated B cells enlist cognate $CD4^+$ T cell help to stimulate clonal expansion (1). Upon activation and proliferation, B cells embark on two distinct differentiation pathways (2). First, the initial production of antibody to a pathogen is accomplished through the differentiation of activated B cells into extrafollicular plasmablasts (3). These short-lived cells are essential in generating low-affinity antibodies early during the infection. However, to generate long-lived humoral immunity, activated B cells must migrate to the germinal center, undergo affinity maturation by somatic hypermutation, and undergo isotype switching to produce memory B cells or antibody-secreting plasma cells (ASC) (3). Memory B cells are long-lived and rapidly respond to pathogen re-encounter by proliferating and differentiating into ASC (4). High-affinity, long-lived ASC migrate to the bone marrow, where they continuously secrete antibody and persist for a year or more in mice (5) and decades in humans (6). Therefore, determining the factors that modulate these pathways is critical not only for understanding the generation and maintenance of serological memory but also for optimizing vaccines and therapeutics for autoimmune disorders.

Following antigen receptor ligation, reactive oxygen intermediates (ROI) are generated and required for B cell function (7–9). Previous work has demonstrated that antioxidant treatment decreased lipopolysaccharide (LPS)-induced B cell proliferation *in vitro* (10, 11). Singh and colleagues (12) provided the first piece of evidence that ROI produced following B cell activation are critical for calcium flux and amplification of early BCR-induced signals. Consistent with this idea, B cells deficient in ROI-generating proteins exhibit decreased Syk and Akt phosphorylation following activation (7). Additionally, we have previously shown that the first oxidation product of cysteine, sulfenic acid, is a critical oxidative modification required for the induction of capacitative calcium entry and maintenance of tyrosine phosphorylation following BCR ligation (8). Furthermore, ROI have also been implicated in the humoral immune response *in vivo*. Studies using loss-of-function mutants in the voltage-gated proton channel HVCN1 by Capasso et al. (7) show that ROI act as positive regulators in B cell responses to both T-cell-dependent and -independent model antigens. Taken together, these findings suggest ROI generated following antigen receptor ligation act as positive mediators of B cell responses. In contrast, other studies suggest that the overproduction of ROI associated with chronic viral infections, autoimmune disorders, and cancer plays a role in lymphocyte dysfunction (13–15). Due to the potential role of ROI in pathology, antioxidant supplementation has risen, with 48% of people ingesting one daily (16). The contribution of ROI and antioxidant ingestion to the humoral immune response to a physiological stimulus such as a viral infection is unknown.

In this study, we examined the effect of antioxidant treatment on humoral immune responses during acute viral infection. Mice were treated with Mn(III)tetrakis(4-benzoic acid)porphyrin chloride (MnTBAP), a superoxide dismutase mimetic, from days 0 to 8 during acute lymphocytic choriomeningitis virus (LCMV) infection. We found that early (day 5) expansion of virus-specific IgM and IgG ASC was not affected, but at the peak of the splenic response, MnTBAP-treated mice had 22- and 457-fold-lower numbers of virus-specific IgM and IgG ASC, respectively. When the long-lived ASC in the bone marrow were assessed at day 38, LCMV IgG ASC were found to be decreased 5-fold in the drug-treated mice. Interestingly, the number of virus-specific IgG memory B cells was not affected. In addition, MnTBAP treatment decreased the number of polyfunctional virus-specific $CD4^+$ T

Received 28 September 2012 **Accepted** 7 December 2012
Published ahead of print 19 December 2012
Address correspondence to Jason M. Grayson, jgrayson@wfubmc.edu.

doi:10.1128/JVI.02714-12

cells. The decrease in virus-specific ASC and $CD4^+$ T cells was due to a combination of Bim-mediated cell death and decreased proliferation. Together, these data demonstrate an important role for ROI in controlling the expansion of antigen-specific ASC generated during viral infection and provide a better understanding of how high-dose antioxidant supplementation could affect humoral immune responses following infection and immunization.

MATERIALS AND METHODS

Mice, virus, and infections. Female C57BL/6 mice, 6 to 8 weeks old, were purchased from the National Cancer Institute (Frederick, MD). Bim $(Bcl2l11)^{-/-}$ mice were purchased from Jackson Laboratories. Mice were infected with 2×10^5 PFU of LCMV Armstrong intraperitoneally and used at the time points indicated below. Virus was grown and quantitated as previously described (17). All studies were approved by the Institutional Animal Care and Use Committee (IACUC) of Wake Forest School of Medicine.

MnTBAP treatment. MnTBAP treatment was performed as previously described (18). Briefly, MnTBAP (Calbiochem) was dissolved in 0.1 N NaOH as a 6-mg/ml stock and diluted in sterile phosphate-buffered saline (PBS) to give an intraperitoneal dose of 5 mg/kg of body weight. Four hours later, mice were infected with LCMV Armstrong. A maintenance dose was administered to the mice every 24 h for the duration of treatment.

Cell isolation. Spleens were removed from mice following cervical dislocation. After the spleen was teased apart on a wire mesh screen, red blood cells were osmotically lysed using ACK lysis buffer (Lonza). Splenocytes were resuspended in complete medium containing RPMI 1640 supplemented with 10% fetal calf serum (FCS; HyClone), L-glutamine (HyClone), penicillin-streptomycin (Cellgro), nonessential amino acids (Gibco), and 2-mercaptoethanol (Gibco). To isolate bone marrow cells, both femurs were flushed with complete medium. Red blood cells were osmotically lysed as described above, and then cells were washed and counted.

Surface and intracellular staining. In this study, the following antibodies were used: rat anti-mouse CD4-peridinin chlorophyll protein (CD4-PerCP), rat anti-mouse CD44-allophycocyanin (CD44-APC), rat anti-mouse CD62L-APC-Cy7, rat anti-mouse CXCR5-biotin, rat anti-mouse GL7-fluorescein isothiocyanate (GL7-FITC), rat anti-mouse CD138-phycoerythrin (CD138-PE), rat anti-mouse B220-APC-Cy7, rat anti-mouse B220-APC, rat anti-mouse CD19-APC, hamster anti-mouse PD-1-PE, hamster anti-mouse CD95-PE, anti-mouse CD150-Pacific blue surface, anti-mouse IgD-eFluor 450, rat anti-mouse gamma interferon (IFN-γ)-FITC, rat anti-mouse tumor necrosis factor alpha (TNF-α)-PE, and rat anti-mouse interleukin 2 (IL-2)-APC. All antibodies were purchased from BD Pharmingen except for CD19, IgD (eBioscience), and CD150 (BioLegend). Surface staining was performed by incubating cells in a 1:100 dilution of antibody in 2% FACS buffer (PBS plus 2% FCS) for 30 min on ice. Cells were washed three times with FACS buffer and fixed in 2% paraformaldehyde (Sigma-Aldrich, St. Louis, MO). After three washes, intracellular cytokine staining was performed using the BD Cytofix/Cytoperm kit according to the manufacturer's protocol. Samples were acquired on a BD FACSCanto instrument and analyzed using FlowJo software (TreeStar, San Francisco, CA).

For CXCR5, secondary stains were performed. Briefly, cells were incubated in a 1:100 dilution of CXCR5-biotin in FACS buffer for 30 min at room temperature. Following three washes with FACS buffer, cells were stained with PE-Cy7-labeled streptavidin (Invitrogen) for 30 min on ice. Cells then were washed three times with FACS buffer and fixed in 2% paraformaldehyde.

Intracellular IL-21 staining was performed following surface staining as previously described by Johnston et al. (19). Briefly, samples were fixed and permeabilized using BD Cytofix/Cytoperm and incubated with recombinant human IL-21 R subunit Fc chimera (R&D Systems) for 60 min on ice. After two washes, samples were stained with APC-conjugated $F(ab')_2$ fragment goat anti-human IgG Fcγ for 30 min on ice. Samples were washed twice with PermWash buffer and twice with FACS buffer and then fixed in 2% paraformaldehyde.

Enzyme-linked immunospot (ELISPOT) analysis. IgM and IgG LCMV-specific ASC were quantified using nitrocellulose bottom 96-well plates (Millipore, Billerica, MA) coated with LCMV-infected BHK cell lysate as previously described (20). Briefly, coated plates were washed with PBS containing 0.1% Tween 20 (PBS-T) followed by three washes with PBS. The plates were blocked with complete medium for 1 h at room temperature. Threefold dilutions of cells were incubated on the blocked plate for 5 h at 37°C. Following washes, samples were incubated with biotin-conjugated goat anti-mouse IgM(μ) or IgG(γ) (Invitrogen) for a minimum of 12 h at 4°C. The plates were washed with PBS-T and incubated with horseradish peroxidase-conjugated avidin-D (Vector Laboratories) for 1 h at room temperature. After washes, the plates were developed using hydrogen peroxide chromogen substrate. The membranes were dried, and spots were enumerated.

Antibody titer. At the time points indicated below, serum from infected mice was collected, and the LCMV-specific antibody titer was quantified by enzyme-linked immunosorbent assay (ELISA) as previously described (17). The LCMV-specific antibody titer is expressed as the reciprocal of the highest dilution showing a reading for optical density at 492 nm (OD_{492}) greater than three times the average OD_{492} reading of background levels.

Antibody affinity. LCMV-specific IgG affinity was determined by a modification of an ELISA method previously described by Bates et al. (21). Briefly, 96-well plates were coated overnight with LCMV-infected BHK cell lysate. The plates were washed three times with PBS containing 0.05% Tween 20 and blocked with 200 μl of PBS supplemented with 10% FCS for 2 h at room temperature. Following three washes, serum samples were added to the wells and incubated overnight at 4°C. The wells were washed five times, and various concentrations of sodium thiocyanate (NaSCN) were added to the plate for 15 min. Samples were washed and incubated with horseradish peroxidase-conjugated anti-mouse IgG (SouthernBiotech) for 2 h at room temperature. Wells were developed with tetramethylbenzidine (Sigma-Aldrich) for 30 min. The reaction was stopped with 2 N H_2SO_4, and absorbance was measured at 450 nm. The affinity was defined as the concentration of NaSCN required to produce a 50% reduction in absorbance. Preliminary studies were conducted in order to determine that the optimal serum dilution was 1:51,200. At this dilution, no protein precipitate formed during the development of the assay.

Quantification of LCMV-specific memory B cells. LCMV-specific memory B cells were quantified by a modification of a limiting dilution method described previously (22). Briefly, 5-fold dilutions of splenocytes from infected mice were tested in 12-well replicates. Splenocytes were cultured in a 96-well flat-bottom plate for 5 days at 37°C in the presence of 1×10^6 irradiated (1,200 rads) sex-matched feeder splenocytes, 0.6 μg of R595 lipopolysaachride (Alexis Biochemicals), and 20 μl of concanavalin A supernatant in complete medium for a total volume of 200 μl. After 5 days of polyclonal stimulation, cells were harvested, washed, and transferred to a nitrocellulose bottom 96-well plate coated with LCMV-infected BHK cell lysate. LCMV-specific ELISPOT assays were performed as previously described (20).

BrdU labeling. Mice were administered 0.8 mg/ml of bromodeoxyuridine (BrdU) in the drinking water beginning at day 6 of LCMV Armstrong infection. BrdU staining was performed as previously described by Tebo et al. (23). Samples were acquired on a BD FACSCanto instrument and analyzed using FlowJo software.

Statistical analysis. Data from vehicle- and MnTBAP-treated mice were analyzed using a two-tailed Student *t* test. A P value of ≤ 0.05 was considered significant.

RESULTS

Administration of MnTBAP decreases ROI levels in activated/memory phenotype B cells during an acute viral infection. Previous studies have determined that superoxide generated follow-

ing naïve BCR ligation is critical for cysteine oxidation (8) and signal transduction pathways (7). Therefore, we hypothesized that following *in vivo* activation, B cells generate ROI, which regulate their responses. To address this hypothesis, we wanted to determine if ROI levels increase in B cells following *in vivo* activation with a physiological stimulus such as viral infection. Superoxide production was assessed using the fluorescent dye dihydroethidium (HE), a cell-permeant dye that upon oxidation intercalates into DNA. Unactivated B cells were identified as $B220^+$ IgD^+ cells, while activated/memory phenotype B cells were identified as $B220^+$ IgD^{lo} cells (19). Figure 1A demonstrates that unactivated B cells from naïve mice contain basal levels of superoxide, with a mean fluorescence intensity (MFI) of 3,225. However, on day 8 after LCMV infection, superoxide levels in activated/memory phenotype B cells had increased to an MFI of 6,377 (Fig. 1B). In contrast, when we assessed the superoxide production in MnTBAP-treated mice on day 8 postinfection, superoxide levels in activated/memory phenotype B cells were found to be modestly reduced, to an MFI of 5,579 (Fig. 1B). When data from multiple mice were normalized to unactivated, naïve B cells, treatment with MnTBAP modestly reduced the levels of superoxide in activated/memory phenotype B cells (fold increases were 1.90 for vehicle-treated cells and 1.50 for MnTBAP-treated cells) (Fig. 1C). Thus, superoxide production increases in B cells following *in vivo* activation during acute viral infection, and MnTBAP treatment lowers the level of ROI produced.

The expansion of virus-specific antibody-secreting cells, but not memory B cells, is reduced in MnTBAP-treated mice. Because ROI production following receptor ligation promotes signal transduction, we hypothesized that lowering ROI with MnTBAP would decrease B cell responses following viral infection. To address this hypothesis, we administered the antioxidant MnTBAP to mice infected with LCMV Armstrong from days 0 to 8 postinfection. In both vehicle- and MnTBAP-treated mice, LCMV Armstrong induces an acute infection that peaks to similar levels at day 3 and is cleared in 9 to 10 days (18). It also induces a large expansion of B cells that differentiate into antigen-specific ASC which secrete virus-specific antibody for the life of the animal (5). The initial ASC response occurs in the spleen at day 8 postinfection; however, by day 30, 90% of the cells will home to the bone marrow (5). Early during infection, on day 5, vehicle- and drug-treated mice had similar numbers of virus-specific IgM and IgG ASC in the spleen (Fig. 2A and B). At the peak of the response, on day 8 postinfection, antigen-specific IgM and IgG ASC were decreased 22- and 457-fold, respectively, compared to levels in control mice. Virus-specific ASC located in the blood and lymph nodes were also reduced in the MnTBAP-treated mice, suggesting that the cells were not localized to a different tissue (data not shown). ASC were lower at day 10 postinfection; however, the virus-specific IgM and IgG ASC responses in the spleen were similar in the two groups by day 15 postinfection. When the long-lived LCMV-specific ASC population was analyzed on day 38 postinfection, there was a significant reduction in the IgG (5-fold) but not the IgM response in MnTBAP-treated mice (Fig. 2C and D). Additionally, we detected similar kinetics and reductions in the polyclonal plasmablast ($CD19^{hi\text{-}int}$ $B220^{hi\text{-}int}$ $CD138^+$ IgD^-) pool between vehicle- and MnTBAP-treated mice (Fig. 2E). Because virus-specific ASC were decreased with antioxidant treatment, we determined whether total IgG ASC was altered. After 8 days of vehicle or MnTBAP treatment of uninfected mice, there was no significant

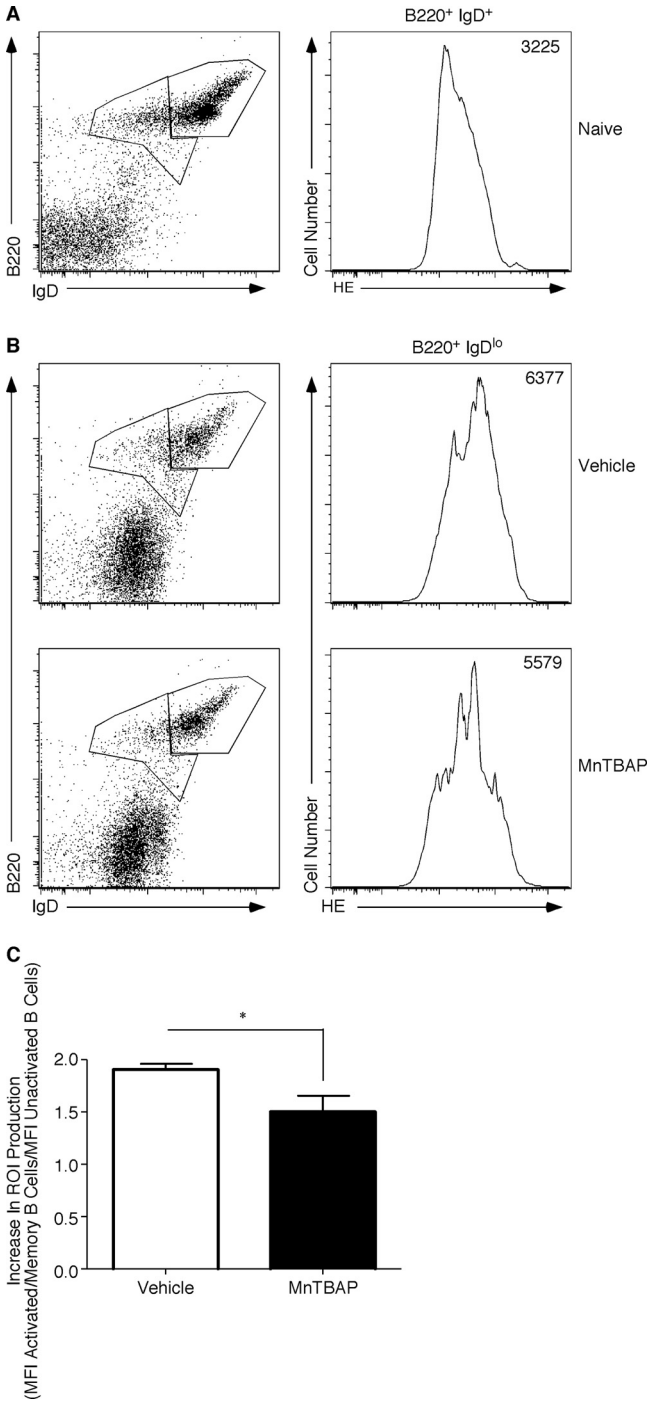

FIG 1 Treatment with MnTBAP reduces superoxide levels in activated B cells. Splenocytes from naïve C57BL/6 mice (A) or those infected with 2×10^5 PFU of LCMV Armstrong 8 days prior and treated with either vehicle or 5 mg/kg of MnTBAP (B) were incubated with HE and stained with anti-B220 and anti-IgD antibodies. The HE levels are plotted as histograms, with the MFI indicated in the upper right corners of the plots. (C) Quantification of HE levels in activated/memory phenotype B cells from multiple mice was done by dividing the HE MFI of activated memory phenotype B cells ($B220^+$ IgD^{lo}) in infected mice by the HE MFI of unactivated B cells ($B220^+$ IgD^{hi}) in naïve mice. Six mice were analyzed in a minimum of two independent experiments. *, significant difference between vehicle- and MnTBAP-treated mice; $P \leq 0.05$.

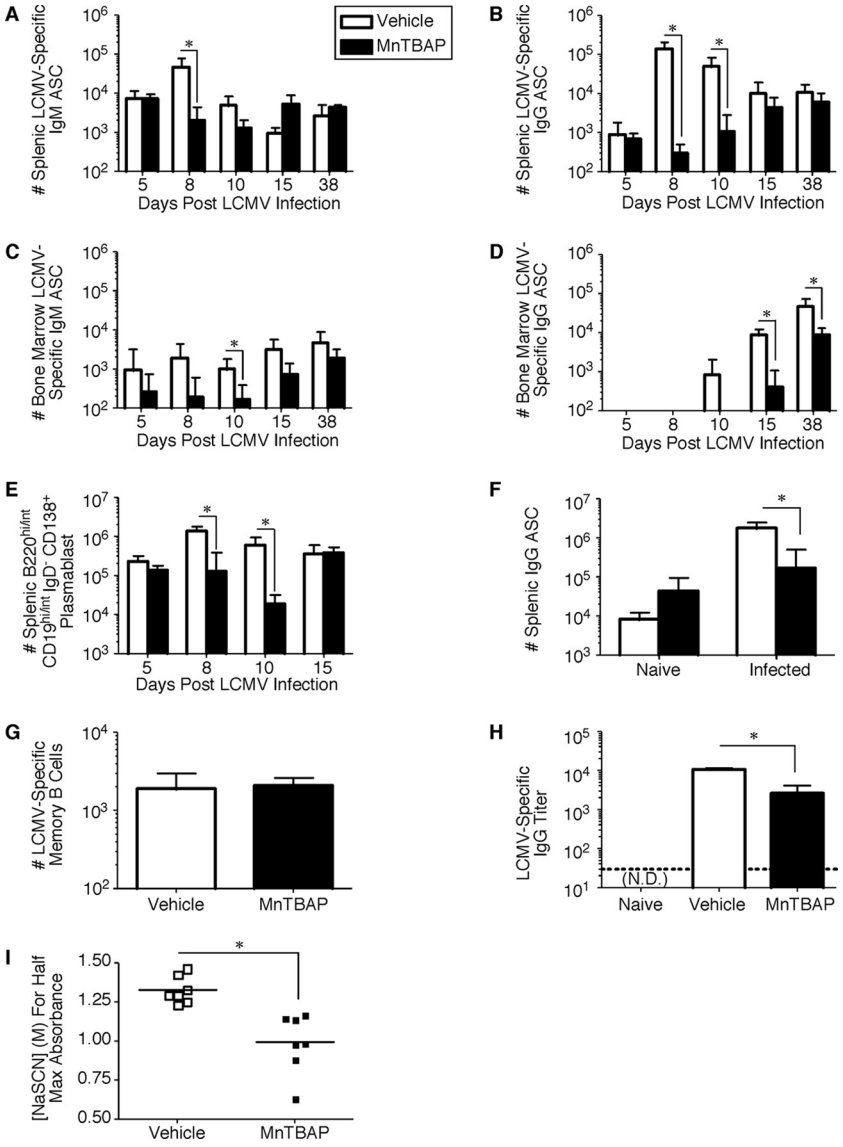

FIG 2 MnTBAP treatment results in decreased expansion of virus-specific IgM and IgG ASC during acute viral infection. C57BL/6 mice were treated with vehicle or 5 mg/kg of MnTBAP. Four hours later, mice were infected with 2×10^5 PFU of LCMV Armstrong. A maintenance dose of vehicle or MnTBAP was administered every 24 h for 8 days. At the indicated time points, mice were sacrificed and the numbers of virus-specific IgM (A and C) and IgG (B and D) ASC in the spleen and bone marrow were quantitated by ELISPOT assay. (E) Quantification of the number of plasmablasts in vehicle- and MnTBAP-treated mice following staining with anti-B220, anti-CD19, anti-IgD, and anti-CD138. (F) Naïve or LCMV-infected mice received a daily dose of vehicle or MnTBAP every 24 h for 8 days. On day 8, mice were sacrificed and spleens were removed. The total IgG ASC were quantitated by ELISPOT assay. (G) The number of LCMV-specific IgG memory B cells was quantified by limiting dilution assay at day 38 postinfection in vehicle- and MnTBAP-treated mice. (H) Serum virus-specific IgG antibody titer was determined on day 38 postinfection by ELISA. The dashed line represents the limit of detection. N.D., not detectable. (I) Affinity was determined by ELISA and was quantified as the concentration of NaSCN required to reduce the absorbance of serum virus-specific IgG by 50%. The averages and standard deviations are shown. Five to nine mice were analyzed in a minimum of two independent experiments. *, significant difference between vehicle- and MnTBAP-treated mice; $P \leq 0.05$.

difference in the number of polyclonal ASC (Fig. 2F). During infection, the total number of IgG-secreting ASC increased to 1.72×10^6 in vehicle-treated mice, and this was reduced 4-fold following MnTBAP administration. Taken together, these data suggest that MnTBAP is not inherently cytotoxic to ASC.

In addition to examining the number of LCMV-specific ASC, we determined whether MnTBAP treatment affected the generation of virus-specific IgG memory B cells. These quiescent and recirculating cells respond rapidly to antigen re-encounter by differentiating into virus-specific ASC (5). Interestingly, the numbers of antigen-specific IgG memory B cells were equivalent between the two groups at day 38 postinfection (Fig. 2G). Therefore, treatment with MnTBAP reduces the number of antigen-specific ASC while having no effect on the generation of memory B cells.

MnTBAP treatment reduces the titer and affinity of virus-specific IgG antibody. The ability of ASC to produce antibodies is often the immune system's first line of defense to an invading pathogen. As shown in Fig. 2H, we compared the virus-specific

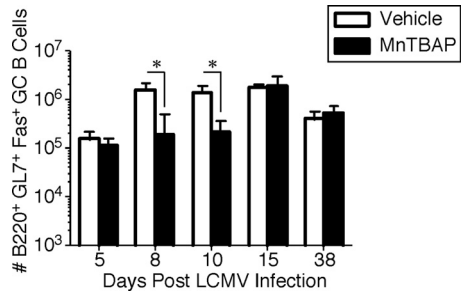

FIG 3 MnTBAP treatment decreases the number of germinal center B cells. C57BL/6 mice were treated with either vehicle or 5 mg of MnTBAP/kg. After 4 h, mice were infected with 2×10^5 PFU of LCMV Armstrong. A maintenance dose was administered every 24 h for 8 days. At the indicated time points, mice were sacrificed, the spleen was removed, and cells were stained with anti-B220, anti-GL7, and anti-Fas. The numbers of $B220^+$ $GL7^+$ Fas^+ germinal center B cells were quantitated, and the averages and standard deviations are shown. Five to six mice were examined in a minimum of two independent experiments. *, significant difference between vehicle- and MnTBAP-treated mice; $P \leq 0.05$.

antibody titers in vehicle- and MnTBAP-treated mice at day 38 postinfection. In vehicle-treated mice, the serum LCMV-specific IgG titer reached 10,000. When titers in MnTBAP-treated mice were examined, they were found to be reduced to 2,500. In addition to total titer, it is critical to measure the affinity of the antibodies generated. On day 38 postinfection, serum samples from vehicle- and MnTBAP-treated mice were collected, and antibody affinity was determined by the concentration of sodium thiocyanante (NaSCN) required to reduce the antigen-bound antibody absorbance by 50% as measured by ELISA. The average LCMV-specific antibody affinity from vehicle-treated mice was 1.3 M NaSCN, while samples from MnTBAP-treated mice had a significant reduction (0.99 M) in antibody affinity (Fig. 2I). Thus, MnTBAP treatment reduces the affinity and titer of LCMV-specific IgG antibody.

MnTBAP treatment decreases the number of germinal-center B cells. Previous studies have shown that germinal center B cell formation is critical to the differentiation of long-lived, high-affinity ASC (24). Because MnTBAP treatment decreased the overall titer and affinity of the anti-LCMV antibody, we determined whether the number of germinal center B cells was altered. Figure 3 shows that early during infection, on day 5, the numbers of germinal center B cells ($B220^+$ $GL7^+$ Fas^+) were roughly equivalent in the two groups of mice (1.53×10^5 for vehicle versus 1.14×10^5 for MnTBAP). However, in vehicle-treated mice, the number of germinal center B cells expanded to 1.36×10^6 cells at day 8 and remained elevated through day 15 postinfection. This result contrasts with that for the MnTBAP-treated mice, which had a substantial reduction in germinal B cells at days 8 and 10 postinfection. However, by day 15 postinfection, germinal center B cell numbers in MnTBAP-treated mice reached a similar peak. By day 38 postinfection, the numbers of germinal center B cells declined and were equivalent between the two groups. Therefore, treatment with MnTBAP alters the number of germinal center B cells and the kinetics of their formation.

Administration of MnTBAP decreases the number of functional virus-specific effector and memory $CD4^+$ T cells. Cognate $CD4^+$ T cell help is required for effective B cell responses to T-cell-dependent antigens such as LCMV. Because the number of virus-specific ASC was decreased, we determined whether $CD4^+$ T cell help was altered in MnTBAP-treated mice. To measure functional $CD4^+$ T cells, we performed intracellular cytokine staining for IFN-γ, TNF-α, and IL-2 following *in vitro* GP61-80 stimulation. Early during the effector response, on day 5, we observed similar percentages of cells producing cytokines in vehicle- and MnTBAP-treated mice (Fig. 4A and B). By day 8 postinfection, 16.03% of $CD4^+$ T cells produced only IFN-γ, 10.6% produced both IFN-γ and TNF-α, and 8.35% produced IFN-γ and IL-2. MnTBAP-treated mice showed a decrease in the percentage of cells producing all cytokines such that only 2.16% produced IFN-γ, 1.28% produced both IFN-γ and TNF-α, and 1.25% produced IFN-γ and IL-2. Similar trends were observed at days 10 and 15 postinfection. Analysis of the memory phase revealed that MnTBAP mice had a decrease in the percentage of cells producing IFN-γ and IL-2. In accordance with the percentage data, we observed similar reductions in the total number of functional $CD4^+$ T cells during the effector (day 8, 13-fold) and memory (day 38, 2-fold) phases in MnTBAP-treated mice (Fig. 4C). Furthermore, MnTBAP-treated mice exhibited a reduction in the percentage of IFN-γ cells also producing TNF-α and IL-2 at day 15 (Fig. 4D and E). Taken together, antioxidant treatment decreases the number and polyfunctionality of antigen-specific effector and memory $CD4^+$ T cells.

Treatment with MnTBAP decreases the number of $CD4^+$ T_{FH} cells. Previous studies have demonstrated the requirement of T follicular helper (T_{FH}) cells for the development and maintenance of germinal center B cells (19, 25, 26). Because the number of germinal center B cells was significantly decreased in MnTBAP-treated mice, we determined whether the number of T_{FH} cells was altered with antioxidant treatment. T_{FH} cells were identified as activated ($CD44^{hi}$ $CD62L^{lo}$) $CD4^+$ T cells that express high levels of CXCR5 and low levels of SLAM (27). Figure 5A shows that the numbers of T_{FH} cells were similar for vehicle- and MnTBAP-treated mice early during infection (day 5). However, at days 8 and 10 postinfection, we detected fewer T_{FH} cells in the drug-treated mice relative to control mice. Similar results were observed when we assessed T_{FH} cells by Bcl6 and CXCR5 staining (data not shown). Prior studies have demonstrated that T_{FH} cells within the germinal center (GC T_{FH}) have a greater ability to provide help to B cells (28, 29). Early during infection, at day 5, vehicle- and MnTBAP-treated mice contained similar numbers of this population in the spleen; however, by days 8 and 10 postinfection, the numbers were significantly decreased, 8.3- and 4.6-fold, respectively, in drug-treated mice (Fig. 5B). Although the numbers were decreased at days 8 and 10 postinfection in MnTBAP-treated mice, this population increased in drug-treated mice to levels similar to those in the control mice by day 15 postinfection.

T_{FH} cell-derived IL-21 is critical for proliferation and survival of germinal center B cells, isotype switching, and ASC differentiation (30, 31). In Fig. 5C, we compared the abilities of $CD4^+$ T cells from vehicle- and MnTBAP-treated mice to produce IL-21 when stimulated with phorbol myristate acetate (PMA) and ionomycin *in vitro*. Early during infection, on day 5, MnTBAP-treated mice had numbers of IL-21-producing $CD4^+$ T cells similar to those of the control mice. At day 8 postinfection, the number of functional cells was significantly reduced in the drug-treated mice (1.28×10^6 for vehicle versus 1.85×10^5 for MnTBAP). Similar trends were observed at day 10 postinfection. However, when we

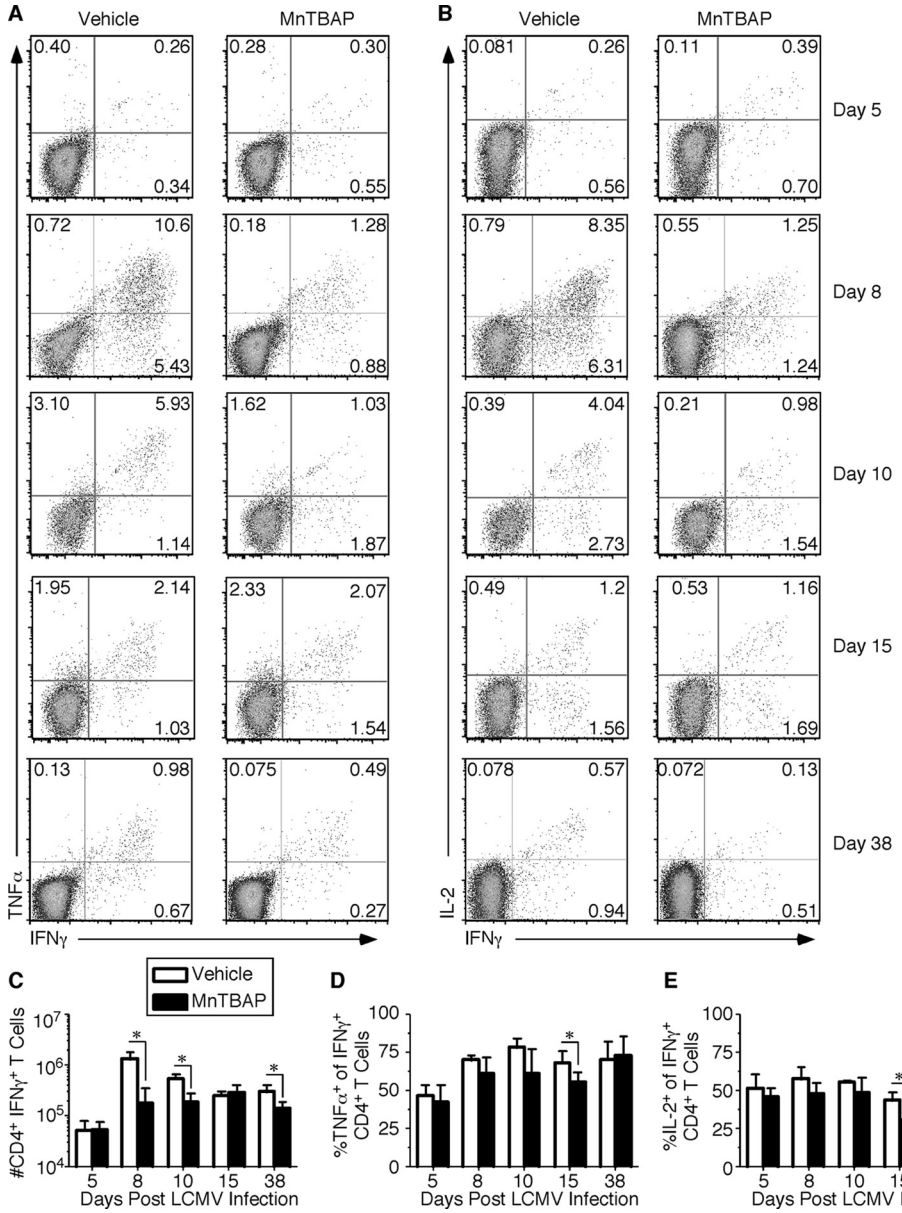

FIG 4 Decreased cytokine production by virus-specific $CD4^+$ T cells from mice treated with MnTBAP. C57BL/6 mice were treated with either vehicle or 5 mg of MnTBAP/kg. After 4 h, mice were infected with 2×10^5 PFU of LCMV Armstrong. A maintenance dose was administered every 24 h for 8 days. At the indicated time points, mice were sacrificed and the spleen was removed. Splenocytes were stimulated with GP61-80 peptide for 5 h at 37°C. Following stimulation, cells were stained with anti-CD4, anti-IFN-γ, and either anti-TNF-α (A) or anti-IL-2 (B). The dot plots are gated on $CD4^+$ T cells, and the numbers in each plot indicate the percentage of $CD4^+$ T cells present in the quadrants. (C) The number of IFN-γ^+ $CD4^+$ T cells was quantitated in the spleen. For each virus-specific $CD4^+$ T cell population, the percentage of IFN-γ^+ cells that produced TNF-α (D) and IL-2 (E) was determined. The averages and standard deviations are plotted. Five to six mice were analyzed in a minimum of two independent experiments. *, significant difference between vehicle- and MnTBAP-treated mice; $P \leq 0.05$.

assessed the cells on day 15 postinfection, we found that the numbers of $CD4^+$ T cells producing IL-21 were similar for the two groups. Taken together, these results demonstrate that antioxidant treatment decreases the number and function of T_{FH} cells at days 8 and 10 postinfection. However, this loss was temporary, because MnTBAP-treated mice recovered by day 15 postinfection.

Decreased expansion of virus-specific ASC and $CD4^+$ T cells is due to decreased proliferation and increased Bim-mediated cell death. Cell number is a balance of proliferation and cell death. While we observed similar numbers of virus-specific ASC and $CD4^+$ T cells in vehicle- and MnTBAP-treated mice at day 5 postinfection, there was a significant reduction in drug-treated mice by day 8. To determine whether proliferation was altered in the MnTBAP-treated mice, we administered 0.8 mg/ml of bromodeoxyuridine (BrdU) in the drinking water of both groups of mice at day 6 postinfection. A mouse receiving water alone was used as a control. This time point was selected because it was an intermediate point between days 5 and 8 postinfection, when we observed a decrease in cell number. Spleens were harvested from mice at day 7 postinfection and stained for surface markers and

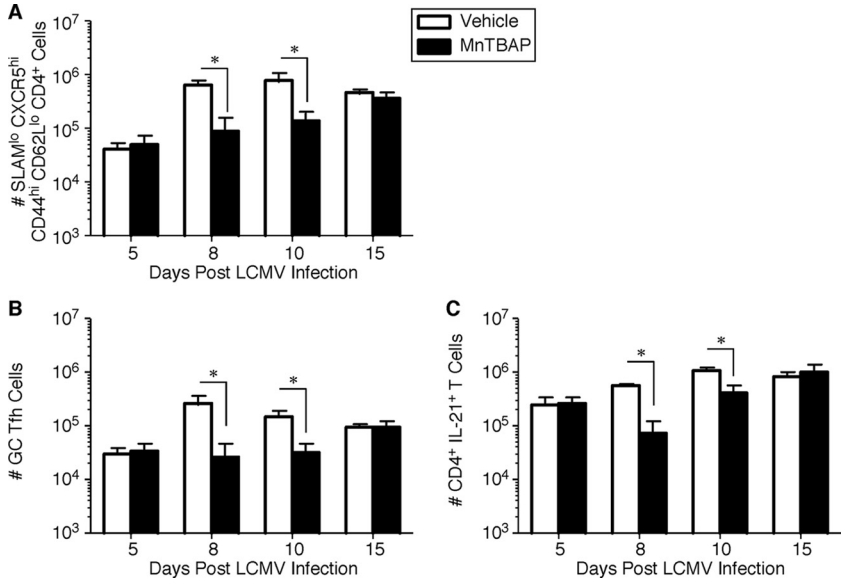

FIG 5 Reduced number of functional T_{FH} cells in mice treated with MnTBAP during an acute viral infection. C57BL/6 mice were treated with either vehicle or 5 mg of MnTBAP/kg. After 4 h, mice were infected with 2×10^5 PFU of LCMV Armstrong. A maintenance dose was administered every 24 h for 8 days. At the indicated time points, mice were sacrificed and the spleen was removed. Splenocytes were stained with anti-CD4, anti-CD44, antiCD62L, and anti-CXCR5 and anti-SLAM (A) or anti-GL-7 (B). The numbers of T_{FH} cells (A) and germinal center (GC) T_{FH} cells (B) were quantitated, and the averages and standard deviations are shown. (C) To determine the effect of MnTBAP administration on IL-21 production by $CD4^+$ T cells, mice were sacrificed at the indicated time points and stimulated with PMA and ionomycin for 4 h at 37°C. Following stimulation, cells were stained with anti-CD4 and IL-21R. The number of IL-21$^+$ $CD4^+$ T cells was quantitated in the spleen, and the averages and standard deviations are shown. Five to six mice were analyzed in a minimum of two independent experiments. *, significant difference between vehicle- and MnTBAP-treated mice; $P \leq 0.05$.

intracellular BrdU. In vehicle-treated mice, 38.6% of plasmablasts were BrdU$^+$, compared to 13.9% in MnTBAP-treated mice (Fig. 6A). Similar trends were observed in the activated $CD4^+$ T cell compartment (47.3% for vehicle versus 16.3% for MnTBAP) (Fig. 6B). Data from multiple mice revealed a significant decrease in the percentages of plasmablasts and activated $CD4^+$ T cells that were BrdU$^+$ in the MnTBAP-treated mice (Fig. 6C). These results indicate that plasmablasts and activated $CD4^+$ T cells in MnTBAP-treated mice underwent reduced proliferation.

In addition to measuring proliferation, we assessed the contribution of cell death by examining whether mice deficient in Bim (*Bcl2l11*), a BH_3-only proapoptotic member of the Bcl-2 superfamily, could rescue the cell number defect we observed in the MnTBAP-treated mice at day 8 postinfection. Wild-type and *Bcl2l11*$^{-/-}$ mice were treated with vehicle or MnTBAP and then infected with LCMV Armstrong. The humoral and cell-mediated responses were measured at day 8 postinfection. As we previously observed, wild-type MnTBAP-treated mice had significant decreases in the numbers of splenic virus-specific IgM and IgG ASC (Fig. 6D) and functional antigen-specific $CD4^+$ T cells (Fig. 6E) compared to vehicle-treated mice. When *Bcl2l11*$^{-/-}$ mice were examined, both the IgM and IgG virus-specific ASC were found to be increased in vehicle-treated mice compared to the levels observed in wild-type animals. Strikingly, loss of Bim rescued much of the decrease in ASC observed at day 8 in MnTBAP-treated mice. Similar trends were observed when we analyzed the number of antigen-specific $CD4^+$ T cells (Fig. 6F). Since the loss of Bim rescued most of the antigen-specific ASC and $CD4^+$ T cells in MnTBAP-treated mice, we wanted to determine whether viral replication was altered. Similar to our prior studies (18), we observed that wild-type vehicle-treated mice had viral titers of 1.5×10^4 PFU/g in their spleens at day 8 postinfection. This contrasted with findings for MnTBAP-treated wild-type mice, in which viral titers were 3.8×10^5 PFU/g. Treatment with MnTBAP delays viral clearance from day 9 to 10 postinfection in wild-type mice (18). When vehicle- and MnTBAP-treated *Bcl2l11*$^{-/-}$ mice were examined, viral titers were found to be 3.2×10^4 and 5×10^4 PFU/g, respectively (Fig. 6G). Importantly, titers were not significantly altered with treatment in *Bcl2l11*$^{-/-}$ mice, demonstrating that the rescue in LCMV-specific ASC was not due to differences in viral load. Taken together, these results demonstrate that the alteration in antigen-specific ASC and activated $CD4^+$ T cells in drug-treated mice is due to a combination of decreased proliferation and increased cell death.

DISCUSSION

In this study, we utilized the antioxidant MnTBAP to examine the role of ROI in the humoral immune response during a viral infection. Here, we report five novel observations. First, in response to viral infection, activated/memory phenotype B cells increased their levels of ROI. Second, antioxidant treatment reduced proliferation and increased Bim-mediated cell death of virus-specific IgM and IgG ASC during the effector phase. Third, antioxidant treatment decreased the number and functionality of virus-specific effector and memory $CD4^+$ T cells. Fourth, MnTBAP treatment decreased the affinity of the anti-LCMV IgG antibody at day 38 postinfection. Fifth, antioxidant treatment had no effect on the number of virus-specific IgG memory B cells generated. Taken together, these results demonstrate that ROI generated in response to an acute viral infection are critical in controlling both the antiviral humoral and $CD4^+$ T cell responses.

What are the roles of ROI in B cell responses? Prior work

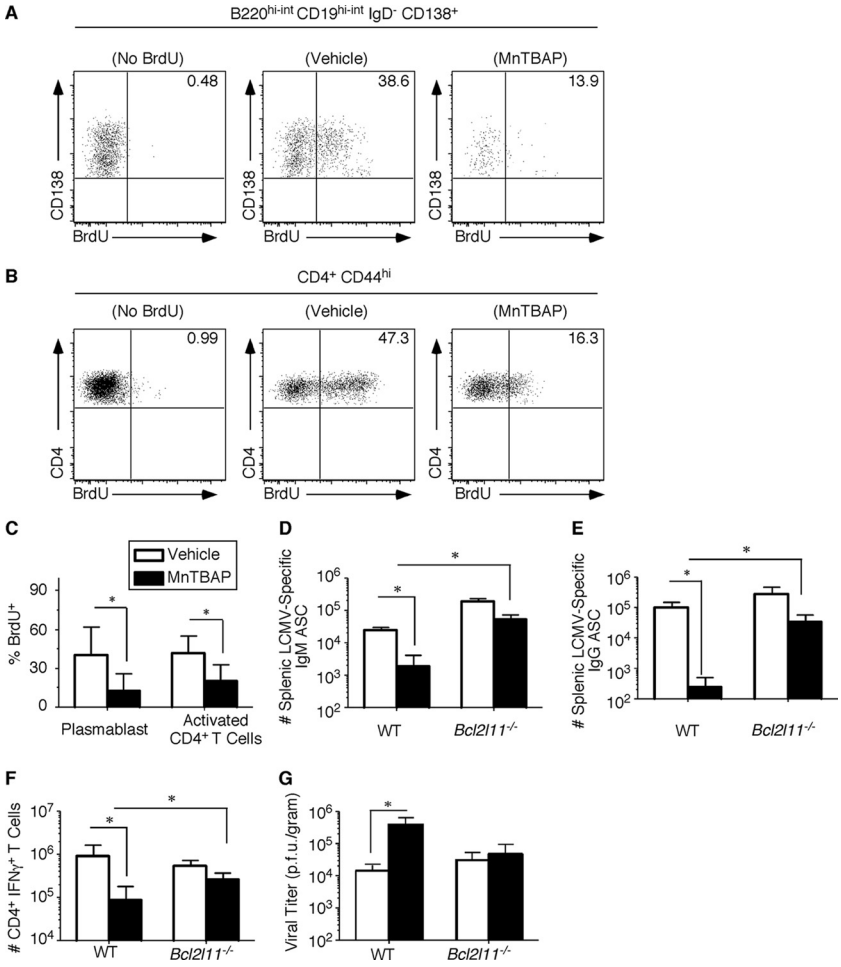

FIG 6 Reduced ASC and $CD4^+$ T cells in MnTBAP-treated mice are due to decreased proliferation and increased Bim-mediated cell death. C57BL/6 mice were treated with either vehicle or 5 mg of MnTBAP/kg. After 4 h, mice were infected with 2×10^5 PFU of LCMV Armstrong. A maintenance dose was administered every 24 h for 8 days. (A) Proliferation was assessed by giving the mice BrdU (0.8 mg/ml) in their drinking water beginning at day 6 postinfection. Mice were sacrificed on day 7 postinfection, and spleens were harvested. Splenocytes were stained with anti-BrdU, anti-CD138 anti-B220, anti-CD19, and anti-IgD (A) or with anti-BrdU, anti-CD4, and anti-CD44 (B). The plots are gated on $B220^{hi\text{-}int}$ $CD19^{hi\text{-}int}$ IgD^- $CD138^+$ plasmablasts (A) or $CD4^+$ $CD44^{hi}$ (B) cells. The numbers in the plots indicate the percentages of plasmablast or activated $CD4^+$ T cells that are $BrdU^+$. The averages and standard deviations are plotted in panel C. C57BL/6 and *Bcl2l11*$^{-/-}$ mice were treated with either vehicle or 5 mg of MnTBAP/kg and infected as described previously. Mice were sacrificed at day 8 postinfection, and the spleens were removed. The numbers of antigen-specific IgM (D) and IgG (E) ASC were quantitated by ELISPOT assay. (F) Splenocytes were stimulated with GP61-80 peptide for 5 h at 37°C. Following stimulation, cells were stained with anti-CD4 and anti-IFN-γ. The number of IFN-γ^+ $CD4^+$ T cells was quantitated in the spleen. (G) Viral titers in the spleens of wild-type (WT) and *Bcl2l11*$^{-/-}$ mice were determined by plaque assay on day 8 postinfection. The averages and standard deviations are shown. Four to six mice were analyzed in a minimum of two independent experiments. *, significant difference between vehicle- and MnTBAP-treated mice; $P \leq 0.05$.

from our laboratory and others has demonstrated that ROI are generated *in vitro* following BCR ligation by antibodies (7–9) or antigen (8). Here, we extend these studies, demonstrating for the first time that ROI are elevated in activated B cells directly *ex vivo* following acute viral infection. There have been conflicting reports regarding the role of these molecules in B cell responses. Addition of antioxidants, which lower ROI, decreases B cell proliferation *in vitro*. This suggests that ROI act in a positive manner to promote B cell proliferation. The role of ROI in B cell responses *in vivo* is less clear. Richards and Clark (9) utilized mice deficient in the gp91 subunit of the NADPH oxidase complex and demonstrated that T-cell-independent responses to model antigens were increased, while T-cell-dependent responses were unaffected. These results suggest that superoxide and other ROI negatively regulate responses. Using HVCN1-deficient mice, which have decreased ROI production, Capasso and colleagues (7) demonstrated that T-cell-dependent responses were decreased following 4-hydroxy-3-nitrophenyl acetyl-keyhole lympet hemocyanin (NP-KLH) immunization. This supports a positive role for ROI in promoting B cell responses *in vivo*. We addressed the role of ROI in a controlled window from days 0 to 8 postinfection through antioxidant administration. Directly *ex vivo*, we observed a 22% decrease in ROI levels in activated B cells and a 457-fold decrease in LCMV-specific IgG-secreting ASC by day 8. Although we were able to modestly reduce ROI in B cells, it is possible that decreasing ROI in other cell types could contribute to the effects we observed. Indeed, in our prior studies of antioxidant treatment on $CD8^+$ T cell responses (18), we demonstrated that MnTBAP treatment lowered ROI in activated T

cells. Interestingly, our data presented here, along with our prior studies of $CD8^+$ T cells (18), demonstrate that the initial phase of the antiviral response (~5 days) is refractory to the effects of antioxidants. This contrasts with *in vitro* studies in which activation and early proliferation are suppressed. One potential explanation is that *in vitro*, superphysiological (millimolar) concentrations of antioxidant are utilized to suppress activation. *In vivo*, it may take several days to reach a concentration of antioxidant sufficient to alter responses. Taken together, the decreased LCMV-specific ASC we observed in MnTBAP-treated mice is consistent with a model in which ROI are positive regulators of B cell responses *in vivo*.

How do ROI positively regulate humoral immune responses *in vivo*? In this study, we observed decreases in LCMV-specific IgG ASC during both the effector and memory phases. Our BrdU incorporation experiments demonstrate that part of the expansion defect is due to decreased proliferation. Multiple checkpoints in the cell cycle are regulated by ROI, including the G_1/S phase and G_2/M transitions (32). Cyclin D1, a critical regulator of the G_0/G_1 transition, is sustained when Nox enzymes are overexpressed under low-serum conditions (33). Treatment with MnTBAP, which lowers superoxide, could lower cyclin D1 levels and decrease the expansion of both antiviral ASC and $CD4^+$ T cells. Similarly, studies by Piganelli and colleagues (34) demonstrated that treatment with AEOL-10113, a superoxide dismutase mimetic, reduced $CD4^+$ T cell proliferation in a diabetes model. Our results extend these findings to an acute infectious disease model and show that expansion of T_{FH} cells is also inhibited by antioxidants. In addition to decreased proliferation, infection of Bim-deficient mice demonstrates that cell death is a major contributor to the expansion defect in ASC of MnTBAP-treated mice. What are the mechanisms by which Bim-mediated cell death is increased with drug treatment? Bim exerts prodeath effects through interactions with prosurvival proteins such as Bcl-2 and Mcl-1. Importantly, we did not observe differences in Bcl-2 levels in activated B cells in MnTBAP-treated mice (data not shown). Previous studies with multiple cell types have demonstrated that the mitogen-activated protein (MAP) kinase cascade is redox regulated (35–39). Additionally, it is well documented that MAP kinase-mediated phosphorylation of Bim_{EL} and its subsequent proteosomal degradation are critical to B and T cell survival upon stimulation (40). Therefore, alterations in MAP kinase signaling in the presence of MnTBAP could decrease Bim_{EL} phosphorylation, increasing its stability and rendering cells more susceptible to death. Lastly, our observations of decreased numbers of antigen-specific ASC, but not memory B cells, in MnTBAP-treated mice are similar to observations following antigen immunization of XBP-$1^{-/-}$ mice (41). Prior studies have clearly documented that oxidation of transcription factors such as NF-κB promotes DNA binding (42, 43). Thus, XBP-1 or other transcription factors known to be critical for ASC generation might be highly sensitive to antioxidants because of potential oxidation sites.

Because of their roles in multiple cell types, there is interest in manipulating ROI for therapeutic benefit. Previous studies determining the efficacy of antioxidants in various disorders, including coronary artery disease and nephropathy, have included administration of 600 mg of *N*-acetylcysteine to patients (44, 45). Based on this dosage, patients typically ingest ~5 to 6 mg per kilogram, which is comparable to the amount of MnTBAP we used in this study. A recent study documented that vitamin C, α-tocopherol, carotenes, selenium, and flavonoids are the most commonly ingested antioxidants in the United States (16). These common antioxidants are beneficial in the treatment and prevention of chronic disorders. For example, there is an inverse relationship between β-carotene and vitamin C ingestion and the incidence of breast cancer in premenopausal women (46, 47). Additionally, studies suggest that diets rich in flavonoids reduce the risk of cardiovascular disease in humans and rodent models (48, 49). Due to positive effects in various disease models, there are currently 1,986 clinical trials using antioxidants (www.clinicaltrials.gov). However, while antioxidant ingestion may play a role in the prevention of chronic disorders, our results have important implications for supplementation during acute immune responses. Our study demonstrates that antioxidant with superoxide dismutase activity has a negative effect on virus-specific ASC, antibody titer, and affinity and suggest that antioxidant supplements should be suspended during infection and immunization.

In conclusion, we demonstrate that treatment with the antioxidant MnTBAP reduces the expansion of virus-specific antibody-secreting cells through decreased proliferation and increased cell death during the effector phase. These effects were also evident during the memory phase, in which the number of LCMV-specific ASC was decreased in the bone marrow and the overall antibody titer and affinity were lower. In addition to effects on B cells, antioxidant treatment decreased the expansion of virus-specific effector and memory $CD4^+$ T cells. Our results demonstrate that ROI positively regulate antibody-secreting cell responses during acute viral infection and suggest that antioxidant treatment could benefit diseases in which inappropriate generation of these cells occurs.

ACKNOWLEDGMENTS

This work was supported by NIAID grant RO1-AI068952 to J.M.G. K.E.C. was supported by NIAID grant 5T32AI007401-20.

REFERENCES

1. **Lanzavecchia A.** 1985. Antigen-specific interaction between T and B cells. Nature **314**:537–539.
2. **Jacob J, Kassir R, Kelsoe G.** 1991. In situ studies of the primary immune response to (4-hydroxy-3-nitrophenyl)acetyl. I. The architecture and dynamics of responding cell populations. J. Exp. Med. **173**:1165–1175.
3. **Zotos D, Tarlinton DM.** 2012. Determining germinal centre B cell fate. Trends Immunol. **33**:281–288.
4. **Tangye SG, Tarlinton DM.** 2009. Memory B cells: effectors of long-lived immune responses. Eur. J. Immunol. **39**:2065–2075.
5. **Slifka MK, Antia R, Whitmire JK, Ahmed R.** 1998. Humoral immunity due to long-lived plasma cells. Immunity **8**:363–372.
6. **Slifka MK, Ahmed R.** 1996. Long-term humoral immunity against viruses: revisiting the issue of plasma cell longevity. Trends Microbiol. **4**:394–400.
7. **Capasso M, Bhamrah MK, Henley T, Boyd RS, Langlais C, Cain K, Dinsdale D, Pulford K, Khan M, Musset B, Cherny VV, Morgan D, Gascoyne RD, Vigorito E, DeCoursey TE, MacLennan IC, Dyer MJ.** 2010. HVCN1 modulates BCR signal strength via regulation of BCR-dependent generation of reactive oxygen species. Nat. Immunol. **11**:265–272.
8. **Crump KE, Juneau DG, Poole LB, Haas KM, Grayson JM.** 2012. The reversible formation of cysteine sulfenic acid promotes B-cell activation and proliferation. Eur. J. Immunol. **42**:2152–2164.
9. **Richards SM, Clark EA.** 2009. BCR-induced superoxide negatively regulates B-cell proliferation and T-cell-independent type 2 Ab responses. Eur. J. Immunol. **39**:3395–3403.
10. **Fedyk ER, Borrello MA, Brown DM, Phipps RP.** 1994. Regulation of B cell tolerance and triggering by immune complexes. Chem. Immunol. **58**:67–91.

11. **Hunt NH, Cook EP, Fragonas JC.** 1991. Interference with oxidative processes inhibits proliferation of human peripheral blood lymphocytes and murine B-lymphocytes. Int. J. Immunopharmacol. **13**:1019–1026.
12. **Singh DK, Kumar D, Siddiqui Z, Basu SK, Kumar V, Rao KV.** 2005. The strength of receptor signaling is centrally controlled through a cooperative loop between Ca2+ and an oxidant signal. Cell **121**:281–293.
13. **Cayota A, Vuillier F, Gonzalez G, Dighiero G.** 1996. In vitro antioxidant treatment recovers proliferative responses of anergic CD4+ lymphocytes from human immunodeficiency virus-infected individuals. Blood **87**: 4746–4753.
14. **Kusmartsev S, Nefedova Y, Yoder D, Gabrilovich DI.** 2004. Antigen-specific inhibition of CD8+ T cell response by immature myeloid cells in cancer is mediated by reactive oxygen species. J. Immunol. **172**:989–999.
15. **Perl A, Gergely P, Jr, Banki K.** 2004. Mitochondrial dysfunction in T cells of patients with systemic lupus erythematosus. Int. Rev. Immunol. **23**: 293–313.
16. **Chun OK, Floegel A, Chung SJ, Chung CE, Song WO, Koo SI.** 2010. Estimation of antioxidant intakes from diet and supplements in U.S. adults. J. Nutr. **140**:317–324.
17. **Ahmed R, Salmi A, Butler LD, Chiller JM, Oldstone MB.** 1984. Selection of genetic variants of lymphocytic choriomeningitis virus in spleens of persistently infected mice. Role in suppression of cytotoxic T lymphocyte response and viral persistence. J. Exp. Med. **160**:521–540.
18. **Laniewski NG, Grayson JM.** 2004. Antioxidant treatment reduces expansion and contraction of antigen-specific CD8+ T cells during primary but not secondary viral infection. J. Virol. **78**:11246–11257.
19. **Johnston RJ, Poholek AC, DiToro D, Yusuf I, Eto D, Barnett B, Dent AL, Craft J, Crotty S.** 2009. Bcl6 and Blimp-1 are reciprocal and antagonistic regulators of T follicular helper cell differentiation. Science **325**: 1006–1010.
20. **Slifka MK, Matloubian M, Ahmed R.** 1995. Bone marrow is a major site of long-term antibody production after acute viral infection. J. Virol. **69**: 1895–1902.
21. **Bates JT, Honko AN, Graff AH, Kock ND, Mizel SB.** 2008. Mucosal adjuvant activity of flagellin in aged mice. Mech. Ageing Dev. **129**:271–281.
22. **Crotty S, Kersh EN, Cannons J, Schwartzberg PL, Ahmed R.** 2003. SAP is required for generating long-term humoral immunity. Nature **421**:282–287.
23. **Tebo AE, Fuller MJ, Gaddis DE, Kojima K, Rehani K, Zajac AJ.** 2005. Rapid recruitment of virus-specific CD8 T cells restructures immunodominance during protective secondary responses. J. Virol. **79**:12703–12713.
24. **Vinuesa CG, Linterman MA, Goodnow CC, Randall KL.** 2010. T cells and follicular dendritic cells in germinal center B-cell formation and selection. Immunol. Rev. **237**:72–89.
25. **Nurieva RI, Chung Y, Martinez GJ, Yang XO, Tanaka S, Matskevitch TD, Wang YH, Dong C.** 2009. Bcl6 mediates the development of T follicular helper cells. Science **325**:1001–1005.
26. **Yu D, Rao S, Tsai LM, Lee SK, He Y, Sutcliffe EL, Srivastava M, Linterman M, Zheng L, Simpson N, Ellyard JI, Parish IA, Ma CS, Li QJ, Parish CR, Mackay CR, Vinuesa CG.** 2009. The transcriptional repressor Bcl-6 directs T follicular helper cell lineage commitment. Immunity **31**: 457–468.
27. **Eto D, Lao C, DiToro D, Barnett B, Escobar TC, Kageyama R, Yusuf I, Crotty S.** 2011. IL-21 and IL-6 are critical for different aspects of B cell immunity and redundantly induce optimal follicular helper CD4 T cell (Tfh) differentiation. PLoS One **6**:e17739. doi:10.1371/journal.pone.0017739.
28. **Crotty S.** 2011. Follicular helper CD4 T cells (TFH). Annu. Rev. Immunol. **29**:621–663.
29. **Yusuf I, Kageyama R, Monticelli L, Johnston RJ, Ditoro D, Hansen K, Barnett B, Crotty S.** 2010. Germinal center T follicular helper cell IL-4 production is dependent on signaling lymphocytic activation molecule receptor (CD150). J. Immunol. **185**:190–202.
30. **Konforte D, Simard N, Paige CJ.** 2009. IL-21: an executor of B cell fate. J. Immunol. **182**:1781–1787.
31. **Linterman MA, Beaton L, Yu D, Ramiscal RR, Srivastava M, Hogan JJ, Verma NK, Smyth MJ, Rigby RJ, Vinuesa CG.** 2010. IL-21 acts directly on B cells to regulate Bcl-6 expression and germinal center responses. J. Exp. Med. **207**:353–363.
32. **Chiu J, Dawes IW.** 2012. Redox control of cell proliferation. Trends Cell Biol. **22**:592–601.
33. **Ranjan P, Anathy V, Burch PM, Weirather K, Lambeth JD, Heintz NH.** 2006. Redox-dependent expression of cyclin D1 and cell proliferation by Nox1 in mouse lung epithelial cells. Antioxid. Redox Signal. **8**:1447–1459.
34. **Piganelli JD, Flores SC, Cruz C, Koepp J, Batinic-Haberle I, Crapo J, Day B, Kachadourian R, Young R, Bradley B, Haskins K.** 2002. A metalloporphyrin-based superoxide dismutase mimic inhibits adoptive transfer of autoimmune diabetes by a diabetogenic T-cell clone. Diabetes **51**:347–355.
35. **Buder-Hoffmann S, Palmer C, Vacek P, Taatjes D, Mossman B.** 2001. Different accumulation of activated extracellular signal-regulated kinases (ERK 1/2) and role in cell-cycle alterations by epidermal growth factor, hydrogen peroxide, or asbestos in pulmonary epithelial cells. Am. J. Respir. Cell Mol. Biol. **24**:405–413.
36. **Conde de la Rosa L, Schoemaker MH, Vrenken TE, Buist-Homan M, Havinga R, Jansen PL, Moshage H.** 2006. Superoxide anions and hydrogen peroxide induce hepatocyte death by different mechanisms: involvement of JNK and ERK MAP kinases. J. Hepatol. **44**:918–929.
37. **Griffith CE, Zhang W, Wange RL.** 1998. ZAP-70-dependent and -independent activation of Erk in Jurkat T cells. Differences in signaling induced by H2o2 and Cd3 cross-linking. J. Biol. Chem. **273**:10771–10776.
38. **Guyton KZ, Liu Y, Gorospe M, Xu Q, Holbrook NJ.** 1996. Activation of mitogen-activated protein kinase by H2O2. Role in cell survival following oxidant injury. J. Biol. Chem. **271**:4138–4142.
39. **McCubrey JA, Lahair MM, Franklin RA.** 2006. Reactive oxygen species-induced activation of the MAP kinase signaling pathways. Antioxid. Redox Signal. **8**:1775–1789.
40. **O'Reilly LA, Kruse EA, Puthalakath H, Kelly PN, Kaufmann T, Huang DC, Strasser A.** 2009. MEK/ERK-mediated phosphorylation of Bim is required to ensure survival of T and B lymphocytes during mitogenic stimulation. J. Immunol. **183**:261–269.
41. **Todd DJ, McHeyzer-Williams LJ, Kowal C, Lee AH, Volpe BT, Diamond B, McHeyzer-Williams MG, Glimcher LH.** 2009. XBP1 governs late events in plasma cell differentiation and is not required for antigen-specific memory B cell development. J. Exp. Med. **206**:2151–2159.
42. **Matthews JR, Wakasugi N, Virelizier JL, Yodoi J, Hay RT.** 1992. Thioredoxin regulates the DNA binding activity of NF-kappa B by reduction of a disulphide bond involving cysteine 62. Nucleic Acids Res. **20**: 3821–3830.
43. **Nishi T, Shimizu N, Hiramoto M, Sato I, Yamaguchi Y, Hasegawa M, Aizawa S, Tanaka H, Kataoka K, Watanabe H, Handa H.** 2002. Spatial redox regulation of a critical cysteine residue of NF-kappa B in vivo. J. Biol. Chem. **277**:44548–44556.
44. **Juergens CP, Winter JP, Nguyen-Do P, Lo S, French JK, Hallani H, Fernandes C, Jepson N, Leung DY.** 2009. Nephrotoxic effects of iodixanol and iopromide in patients with abnormal renal function receiving N-acetylcysteine and hydration before coronary angiography and intervention: a randomized trial. Intern. Med. J. **39**:25–31.
45. **Yilmaz H, Sahin S, Sayar N, Tangurek B, Yilmaz M, Nurkalem Z, Onturk E, Cakmak N, Bolca O.** 2007. Effects of folic acid and N-acetylcysteine on plasma homocysteine levels and endothelial function in patients with coronary artery disease. Acta Cardiol. **62**:579–585.
46. **Howe GR, Hirohata T, Hislop TG, Iscovich JM, Yuan JM, Katsouyanni K, Lubin F, Marubini E, Modan B, Rohan T, Toniolo P, Shunzhang Y.** 1990. Dietary factors and risk of breast cancer: combined analysis of 12 case-control studies. J. Natl. Cancer Inst. **82**:561–569.
47. **Zhang S, Hunter DJ, Forman MR, Rosner BA, Speizer FE, Colditz GA, Manson JE, Hankinson SE, Willett WC.** 1999. Dietary carotenoids and vitamins A, C, and E and risk of breast cancer. J. Natl. Cancer Inst. **91**:547–556.
48. **Arai Y, Watanabe S, Kimira M, Shimoi K, Mochizuki R, Kinae N.** 2000. Dietary intakes of flavonols, flavones and isoflavones by Japanese women and the inverse correlation between quercetin intake and plasma LDL cholesterol concentration. J. Nutr. **130**:2243–2250.
49. **Frémont L, Gozzelino MT, Franchi MP, Linard A.** 1998. Dietary flavonoids reduce lipid peroxidation in rats fed polyunsaturated or monounsaturated fat diets. J. Nutr. **128**:1495–1502.